# BUOYANCY EFFECTS IN TURBULENT JET MIXING

Sergiy Gerashchenko & Kathy Prestridge
*Los Alamos National Laboratory, Los Alamos, New Mexico, USA*

*Abstract* Mixing of a turbulent non-compressible jet of heavy fluid ($SF_6$ gas) injected into coflowing air of lower turbulence is studied experimentally in a vertical wind tunnel. Velocity and density fields are measured simultaneously with Particle Image Velocimetry and Planar Laser Induced Fluorescence. The effect of buoyancy is investigated and compared for two Atwood numbers: 0.1 (Boussinesq case) and 0.6 (strongly non-Boussinesq case). In both cases the initial jet volume flow rates are matched. The high Atwood number jet with larger Reynolds number shows reduced lateral spreading compared to the low Atwood number jet with smaller Reynolds number in both velocity and density profiles, indicating stabilizing effect of buoyancy. The PDF of spatial density gradients for the high Atwood number has much stronger non-exponential tails than for the low Atwood number signifying the reduced rate of mixing of the strongly buoyant jet. The other statistical characteristics of the mixing important for modeling these flows such as spreading rate, turbulent mass flux, density weighted Reynolds stress, turbulent kinetic energy flux, and density-specific volume correlation are also examined in the near and far field from the jet.

## Experimental setup and goals

The experiments are being conducted in a 0.5x0.5x5m open circuit low-speed vertical wind tunnel (Figure 1). To investigate the role of buoyancy effects in the jet flow mixing, two Atwood number jets are studied: $At$=0.6, with heavy $SF_6$ mixed with acetone vapor, and $At$=0.1, when air is premixed with acetone vapor. The volume flow rates are matched in each case. The large $At$ number case has also been studied at lower flow rates to measure Reynolds number effects. In each experiment, the jet is injected into the coflowing air of lower turbulence. Two-dimensional velocity and density fields are measured with simultaneous Particle Image Velocimetry (PIV) and Planar Laser Induced Fluorescence (PLIF). The flow is illuminated with a laser light sheet from the side of the vertical tunnel with two wavelengths of an Nd:YAG pulsed laser (266nm for PLIF and 532nm for PIV). Passive tracer particles (fog droplets) and acetone vapor are premixed with the jet flow for PIV measurements and PLIF visualization, shown in Figure 1. Two digital cameras mounted on translational sleds are used to acquire the PIV and PLIF images. Both cameras can be moved along the tunnel to measure time evolution of the mixing.

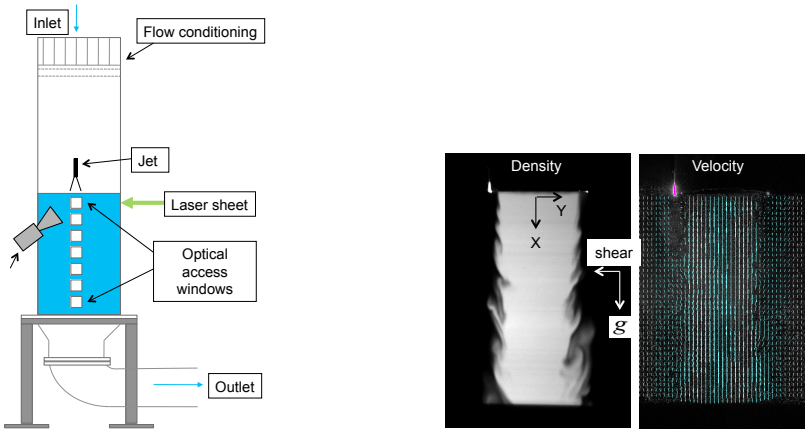


**Figure 1.** Sketch of the experimental setup (left) and jet geometry (right).

| | Atwood Number | Volumetric Flow Rate | Jet Reynolds Number |
|---|---|---|---|
| $SF_6$ case 1 | 0.6 | 6 LPM | 6200 |
| Air case 1 | 0.1 | 6 LPM | 1600 |
| $SF_6$ case 2 | 0.6 | 2.5 LPM | 2400 |

**Table 1.** Experimental cases studied.

Table 1 shows the three experimental cases we have investigated. Jet Reynolds number is based on the initial jet velocity and jet diameter. The choice to match the volumetric flow rates of the air and $SF_6$ jets was made deliberately. Our focus is to investigate buoyancy-driven mixing, so the use of the jet is as a fluid delivery system, and this is not a jet-oriented investigation.

## Results

Figure 2 (left plot) shows the full width of the jet velocity profiles calculated at half maximum for the three cases considered. The large Atwood and Reynolds number case ($SF_6$ case1) has the smallest width in the far field from the jet, indicating the stabilizing effect of buoyancy in the jet spreading. The PLIF images in Figure 2 (right) confirm this, too. There is increased spreading of the air jet in the far field (lowest figure), at $x/d$=14.5.

Figure 3 shows PDFs of the density gradients. The longest non-exponential tails are observed for $SF_6$ case1, which can be interpreted as a reduced rate of mixing at higher Atwood number.

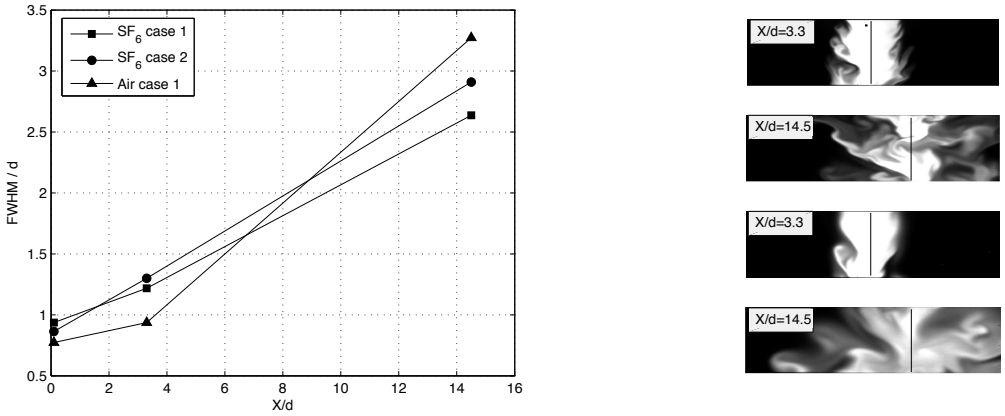


**Figure 2.** FWHM of velocity profiles (left) versus distance from the jet normalized by the jet diameter (d=1.1cm). The three different cases are described in Table 1. PLIF images (right) for $SF_6$ jet case 1 (upper two) and Air jet case 1 (lower two) at different distances from the jet.

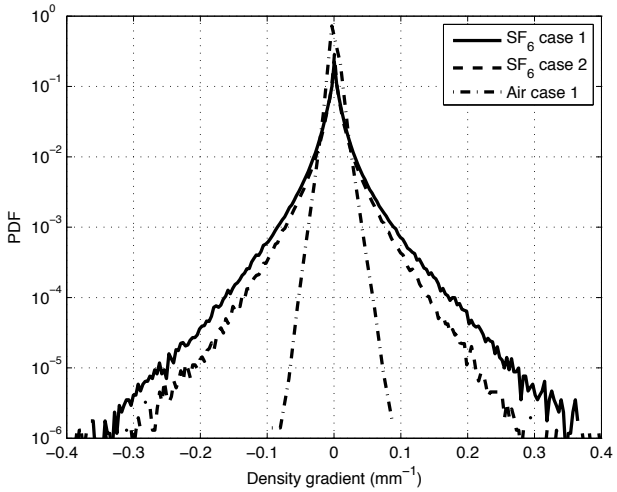


**Figure 3.** PDFs of spanwise density gradient normalized by initial density, at X/d = 14.5.

We will present further analyses of the differences in turbulent mass flux, Reynolds stress, turbulent kinetic energy, and density-specific-volume correlation for the three experimental cases in Table 1. Simulations of these experiments using both Direct Numerical Simulation and Reynolds-Averaged Navier-Stokes simulations are ongoing, and new results will be presented as they become available.